Deep–Sea Research I 175 (2021) 103574

Contents lists available at ScienceDirect

Deep-Sea Research Part I

journal homepage: www.elsevier.com/locate/dsri

# Reef communities associated with 'dead' cold-water coral framework drive resource retention and recycling in the deep sea

Sandra R. Maier [a,*], Furu Mienis [b], Evert de Froe [b], Karline Soetaert [a,c], Marc Lavaleye [b], Gerard Duineveld [b], Olivier Beauchard [a], Anna-Selma van der Kaaden [a], Boris P. Koch [d,e], Dick van Oevelen [a]

[a] Department of Estuarine and Delta Systems, Royal Netherlands Institute for Sea Research (NIOZ-Yerseke), Yerseke, the Netherlands
[b] Department of Ocean Systems, Royal Netherlands Institute for Sea Research (NIOZ-Texel), Den Burg, the Netherlands
[c] Marine Biology Research Group, Department of Biology, Ghent University, Ghent, Belgium
[d] Alfred-Wegener-Institut Helmholtz-Zentrum für Polar- und Meeresforschung, Bremerhaven, Germany
[e] University of Applied Sciences, Bremerhaven, Germany

ARTICLE INFO

*Keywords:*
Carbonate mound
Metabolic activity
Rockall bank
Dissolved organic carbon
Dissolved inorganic nitrogen
Suspension feeder
Video transect

ABSTRACT

Cold-water coral (CWC) reefs create hotspots of metabolic activity in the deep sea, in spite of the limited supply of fresh organic matter from the ocean surface (i.e. phytodetritus). We propose that 'dead' coral framework, which harbours diverse faunal and microbial communities, boosts the metabolic activity of the reefs, through enhanced resource retention and recycling. Analysis of a video transect across a 700-540 m-deep CWC mound (Rockall Bank, North-East Atlantic) revealed a high benthic cover of dead framework (64%). Box-cored fragments of dead framework were incubated on-board and showed oxygen consumption rates of 0.078–0.182 μmol $O_2$ (mmol organic carbon, i.e. OC)$^{-1}$ h$^{-1}$, indicating a substantial contribution to the total metabolic activity of the CWC reef. During the incubations, it was shown that the framework degradation stage influences nitrogen (re)cycling, corresponding to differences in community composition. New (less-degraded) framework released ammonium (0.005 ± 0.001 μmol $NH_4^+$ (mmol OC)$^{-1}$ h$^{-1}$), probably due to the activity of ammonotelic macrofauna. In contrast, old (more-degraded) framework released nitrate (0.015 ± 0.008 μmol $NO_3^-$ (mmol OC)$^{-1}$ h$^{-1}$), indicating that nitrifying microorganisms recycled fauna-excreted ammonium to nitrate. Furthermore, the framework community removed natural dissolved organic matter (DOM) from the incubation water (0.005–0.122 μmol C (mmol OC)$^{-1}$ h$^{-1}$). Additional feeding experiments showed that all functional groups and macrofauna taxa of the framework community incorporated $^{13}$C-enriched ('labelled') DOM, indicating widespread DOM uptake and recycling. Finally, the framework effectively retained $^{13}$C-enriched phytodetritus, (a) by physical retention on the biofilm-covered surface and (b) by biological filtration through suspension-feeding fauna. We therefore suggest that the dead framework acts as a 'filtration-recycling factory' that enhances the metabolic activity of CWC reefs. The exposed framework, however, is particularly vulnerable to ocean acidification, jeopardizing this important aspect of CWC reef functioning.

## 1. Introduction

In the resource-limited deep sea, cold-water corals (CWCs) such as *Lophelia pertusa* (suggested revised name *Desmophyllum pertusum,* Addamo et al., 2016) form flourishing reefs of high biodiversity and biomass (Jonsson et al., 2004; Henry and Roberts, 2007, 2016). These reefs are hotspots of metabolic activity and organic matter mineralization (Van Oevelen et al., 2009). They consume up to 20 times more oxygen ($O_2$) and release around twice as much dissolved inorganic nitrogen (DIN) compared to adjacent soft sediment grounds (Cathalot et al., 2015; De Froe et al., 2019). In the absence of light, CWC reefs depend on food from the ocean surface, such as phytodetritus, i.e. phytoplankton-derived particulate organic matter (POM) (Duineveld et al., 2004; Kiriakoulakis et al., 2005; Van Oevelen et al., 2018a). However, the POM flux to CWC reefs, measured by sediment traps, is orders of magnitude lower than their POM demand to maintain their

* Corresponding author.
*E-mail address:* mail.maier.sandra@gmail.com (S.R. Maier).

https://doi.org/10.1016/j.dsr.2021.103574
Received 29 November 2020; Received in revised form 10 May 2021; Accepted 31 May 2021
Available online 8 June 2021

high metabolic activity (Van Oevelen et al., 2009). Specifically in the temperate North-East Atlantic (Freiwald et al., 2004), where large CWC reefs and mounds are particularly abundant (Roberts et al., 2006), phytodetritus is limited to the productive spring season and supply is low during the remaining part of the year (Duineveld et al., 2004, 2007). To date, it remains unclear how CWC reefs maintain their high metabolic activity under limited resource supply.

Two mechanisms could explain the high metabolic activity of CWC reefs, namely (1) increased POM retention on the reef, through efficient phytodetritus filtration, and (2) recycling of metabolic 'waste' products, such as dissolved organic matter (DOM) and dissolved inorganic nitrogen (DIN). Firstly, the three-dimensional reef framework induces turbulence and may physically trap phytodetritus, which would not settle on a flat seafloor ('physical filtration'; De Haas et al., 2009; Mienis et al., 2009a; Mienis et al., 2019). In addition, suspension feeders trap phytodetritus from the reef-overlaying water ('biological filtration'; Lavaleye et al., 2009; Wagner et al., 2011). Secondly, the reef community may recycle metabolic 'waste' products beyond the productive spring season (Maier et al., 2020a, 2020b). For example, sponges consume (recycle) DOM from coral mucus, transform DOM into particulate sponge detritus (POM), which subsequently feeds reef detritivores ('sponge loop', de Goeij et al., 2013; Rix et al., 2016; Maier et al., 2020b). Furthermore, microbial assemblages of CWCs and sponges oxidize ammonium to nitrate and fix dissolved inorganic carbon (nitrification; Van Duyl et al., 2008; Hoffmann et al., 2009; Middelburg et al., 2015).

Dead framework, i.e. coral skeleton without live coral tissue, is an integral part of a CWC reef (Wilson, 1979; Freiwald and Wilson 1998; Vad et al., 2017). The dead framework could play a central role in the reef metabolic activity (De Froe et al., 2019). While live corals protect their carbonate skeleton against colonisation, the unprotected dead framework offers a hard substrate for a diverse faunal and microbial community (Mortensen et al., 1995; Henry and Roberts, 2007; Van Bleijswijk et al., 2015). The outside of the dead framework (i.e. 'epilithic') is colonized by a thin 'biofilm' (bacteria, fungi, encrusting sponges, hydroids), sessile suspension feeders, mobile detritivores and predators (Henry and Roberts, 2007, 2016; Henry et al., 2013). The inside of the dead framework (i.e. 'endolithic') is inhabited by bioeroding bacteria, fungi, sponges, bryozoans and foraminiferans (Beuck et al., 2010). Appearance, stability and associated communities of dead

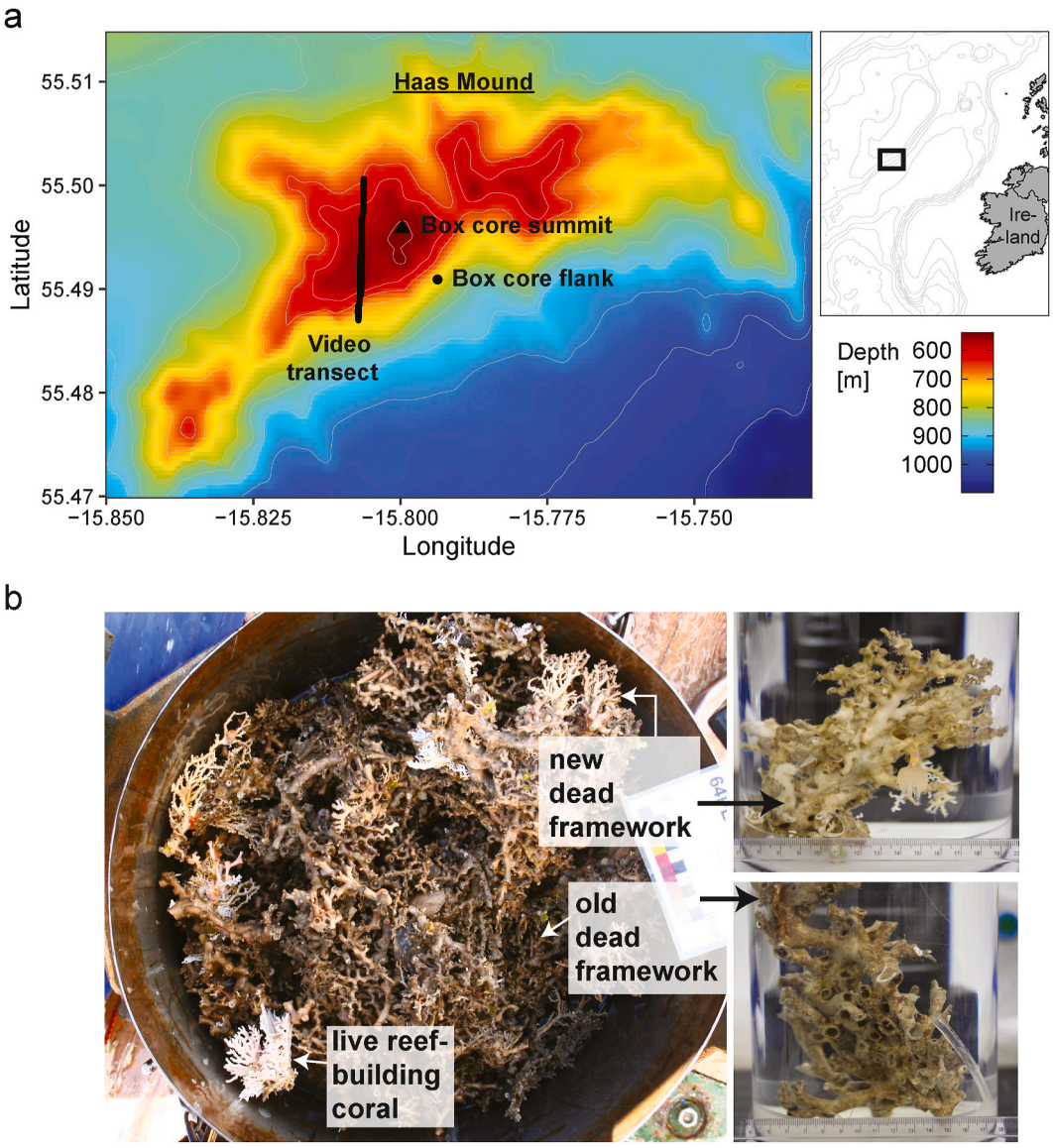


**Fig. 1.** Dead cold-water coral framework studied at Haas Mound. (a) Haas Mound, located at Rockall Bank in the North-East Atlantic. Shown are the south-to-north video transect across Haas Mound and box core sampling sites on the southern flank and summit area. (b) Box core with new dead framework and live reef-building coral situated on top of old dead framework (left picture, arrows) and experimental fragments of new and old dead framework (right pictures).

framework change over time (Freiwald and Wilson, 1998; Beuck and Freiwald, 2005). The early postmortem stage, here called 'new framework', still appears bright, almost white, and shows little bioerosion and biofilm overgrowth (Fig. 1b). In contrast, 'old framework' is typically coated by a dark-brown ferromanganese layer and shows clear signs of bioerosion (traces of borers, pores) and biofilm overgrowth.

The diverse community associated with dead framework might facilitate various trophic pathways (Van Oevelen et al., 2009), promoting resource retention and recycling. So far, however, studies have focussed on the metabolic activity of live corals (Mueller et al., 2014; Middelburg et al., 2015; Maier et al., 2019) and individual macrofauna taxa (Rix et al., 2016; Van Oevelen et al., 2018b; Maier et al., 2020b), while the role of the dead framework remains largely unknown.

We propose that the dead framework boosts the metabolic activity of CWC reefs, by enhancing phytodetritus retention (filtration) and recycling of DOM and DIN. We present a comprehensive study on the dead-framework community at the 700-540 m-deep Haas Mound at the south-eastern flank of the Rockall Bank (Fig. 1, Logachev Mound Province, North-East Atlantic). We investigated (1) the quantitative importance of dead framework on the reef, (2) the composition of the dead-framework community, (3) its metabolic activity, (4) phytodetritus retention (filtration), (5) DOM uptake and (6) (re)cycling of DIN. Firstly, we determined the cover of dead framework, live corals and sediment along a cross-mound video transect (1). Then, we collected dead framework and described the composition and organic carbon content of the associated biota (2). We incubated fragments of dead framework on-board, in natural reef water (Fig. 2a), to measure community oxygen consumption (3), uptake of natural dissolved organic carbon (DOC) (5) and DIN cycling (6). Finally, we carried out a feeding experiment with $^{13}$C-enriched phytodetritus and $^{13}$C-enriched DOM (Fig. 2b). $^{13}$C serves as tracer to follow the incorporation of phytodetritus (4) and DOM (5) by the different community members (tracer-C incorporation).

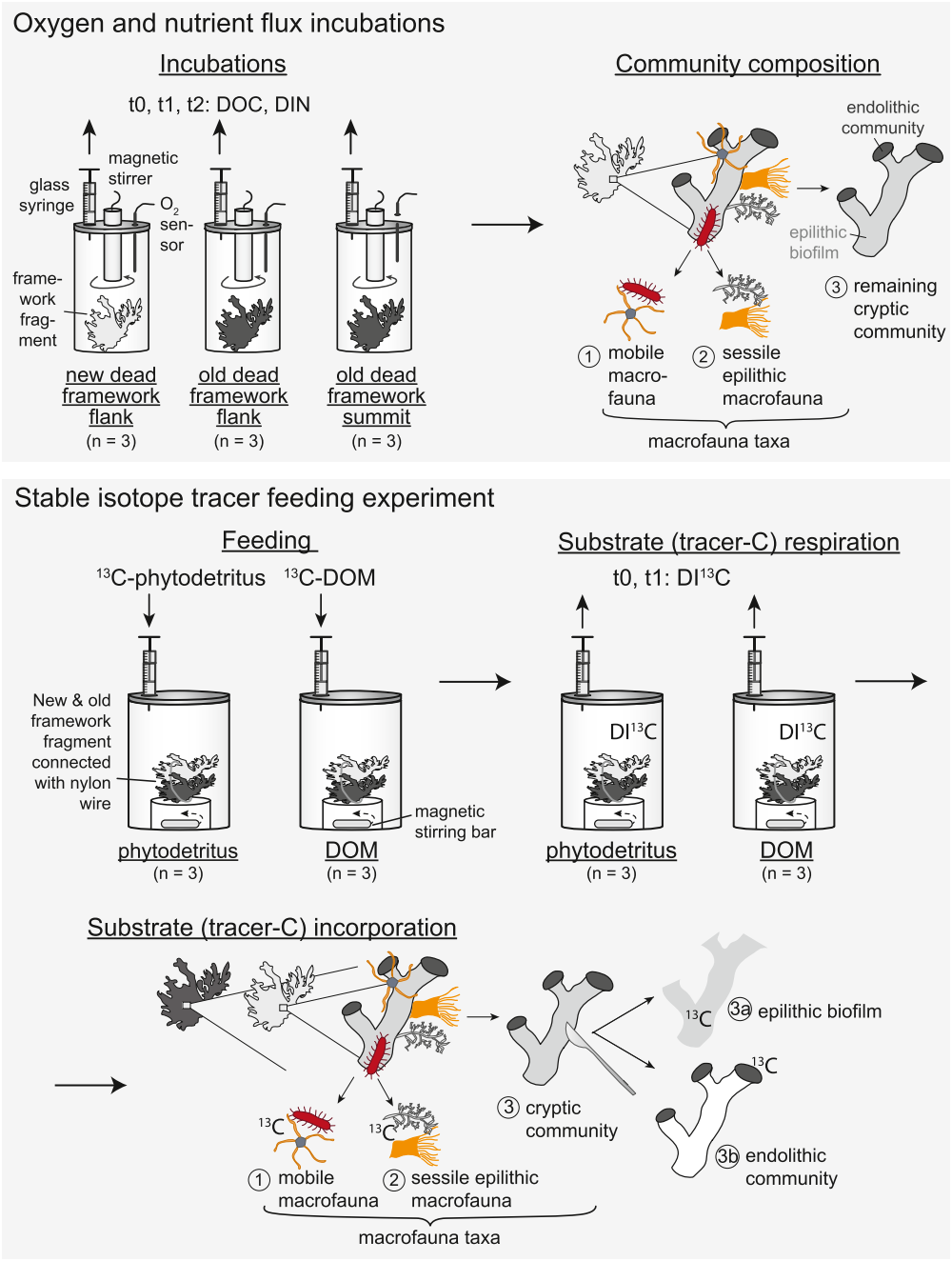


**Fig. 2.** Experimental design. (a) Oxygen and nutrient flux incubations: Fragments of new framework from the mound flank and old framework from the mound flank and summit were individually incubated to measure fluxes of oxygen ($O_2$ sensor), dissolved organic carbon (DOC) and dissolved inorganic nitrogen (DIN). n: number of replicates, t0, t1, t2: water sampling time points. After the incubation, the framework biota were sorted into functional groups (1–3) and macrofauna taxa. (b) Stable isotope tracer feeding experiment: Framework fragments were fed with either $^{13}$C-enriched phytodetritus or $^{13}$C-enriched dissolved organic matter (DOM). $^{13}$C served as a tracer for substrate (phytodetritus/DOM) utilization, i.e. respiration, measured in incubations via production of $^{13}$C-enriched dissolved inorganic carbon (DI$^{13}$C), and incorporation, measured via $^{13}$C appearance in the community functional groups (1–3) and macrofauna taxa.

## 2. Materials and methods

### 2.1. Cross-mound video transect

Haas Mound (700-540 m depth, Fig. 1a) is the largest carbonate mound of the Logachev CWC province. A detailed description of the local environmental conditions is provided by De Froe et al. (2019). During the *RV Pelagia* cruise 64PE360 in October 2012, a video transect was recorded across Haas Mound with a towed camera system from the NIOZ (Royal Netherlands Institute for Sea Research). The camera system has two parallel laser pointers, which mark a fixed difference of 30 cm on the video frames. The 94 min recording covered a linear transect distance of 1553 m, calculated from the transect start and end coordinates with the Haversine formula in R4.0.0 (R Core Team, 2020; package geosphere, Hijmans et al., 2015). Every 1500th still frame was imported into Adobe Photoshop 2020, which resulted in approximately one still frame per 30 s of video time or one every 8.3 m of distance. Each still frame covered an area of $2.8 \pm 1.5$ $m^2$ (mean ± standard deviation), which was calculated from the known distance between the two laser dots and was measured in Photoshop. All 187 still frames were manually analysed in Photoshop (Van der Kaaden, 2021; see examples in Supplementary Figure A.1), for percent benthic cover of (a) live reef-building corals, (b) new dead framework (i.e. early postmortem), (c) old dead framework, (d) sediment plus coral rubble, (e) large erect sponges and (f) other macro- or megafauna (e.g. fish, sea urchins, crabs and sessile taxa besides sponges and reef-building corals). The terms 'new' and 'old' framework are used for visually different stages of framework degradation (Freiwald and Wilson, 1998), although the framework age was not determined here. Coral rubble represents small pieces of dead framework that do not form a three-dimensional structure above the sediment surface.

### 2.2. Framework collection

Dead framework (with the associated biota) was collected from Haas Mound during the *RV Pelagia* cruise 64PE420 in May 2017 with a NIOZ-designed box corer (55 cm high × 50 cm wide, Fig. 1b). The box corer has a trip valve that seals the undisturbed framework sample in its surrounding overlying bottom water while retrieving. Two box cores were taken for the incubation experiment, one at the southern flank of Haas Mound at 643 m depth (Fig. 1a, N 55° 29.45′, W 15° 47.63′), and one at the mound summit area at 540 m depth (N 55° 29.75′, W 15° 47.98′). For the stable isotope tracer feeding experiment, two box cores were taken at the mound flank at 648 m depth (N 55° 29.45′, W 15° 47.64'). On board, the framework was immediately placed into 100 L-maintenance tanks in a thermo-controlled room (8.5 °C). The maintenance tanks contained 0.35 µm-filtered reef water, collected 10 m above the reef with Niskin bottles. Submersible pumps maintained water circulation. The framework was sorted in fragments of new and old framework, while remaining submersed. The summit box core only contained old framework.

### 2.3. Oxygen and nutrient flux incubations

Triplicate, similar-sized fragments of new framework from the mound flank and old framework from the mound flank and summit (111 ± 49 mL, 181 ± 35 g dry mass, Fig. 1b) were individually incubated on board in 0.35 µm-filtered reef water for 41–52 h. Incubations were done in two incubation runs (Supplementary Table A.3) within one day of framework collection. Duplicate controls of 0.35 µm-filtered reef water were run in parallel to measure planktonic oxygen and nutrient fluxes. Incubations were performed in closed, bubble-free 4.83 L-plexiglass chambers in a dark thermo-controlled room (8.5 °C, Fig. 2a). A magnetic stirrer in the chamber lid ensured a well-mixed environment. A FireSting optode (TeX4, Pyro Science) continuously recorded the oxygen ($O_2$) concentration. At three time points (t0 = start, t1 = 23–37 h, t2 = 41–52 h), water samples were taken with a glass syringe (cleaned with 2 %-hydrochloric acid) from each chamber, for the analysis of dissolved organic carbon (DOC) and dissolved inorganic nitrogen (DIN, here ammonium and nitrate; nitrite fluxes were not detectable and are therefore not reported). After the t0-sampling, the chamber was refilled with 0.35 µm-filtered reef water. DOC and DIN were likewise measured in the refill water. To avoid DOC contamination during the incubation, water was not replaced after the t1-sampling, and therefore, the oxygen measurement was stopped at this time point. DOC samples were filtered over combusted glass fiber filters (GF/F, ca. 0.7 µm pore size) in 40 mL acid-cleaned and combusted amber vials, acidified to a pH of ~2 with concentrated hydrochloric acid (HCl) and stored at 4 °C in the dark. The DOC concentration was measured via high-temperature catalytic oxidation on a Shimadzu TOC-VCPN analyser, calibrated with certified reference material (Hansell Laboratory). DIN samples were filtered over 0.45 µm-membrane filters in 5 mL-polyethylene vials and stored frozen (−20 °C). Ammonium and nitrate concentrations were analysed on a SEAL QuAAtro segmented continuous flow analyser. Fluxes of $O_2$, DOC, ammonium and nitrate were calculated by linear regression of the respective concentrations over time, and corrected for the fluxes in the control incubations (Supplementary Table A.3). Fluxes were standardized to the organic carbon content of the framework (OC). To facilitate comparability with other studies, we further report fluxes standardized to framework dry mass (DM) and framework volume within Supplementary Tables A.1 and A.3.

### 2.4. Framework community composition

After the incubation, the volume of the framework fragments was measured (on board) via water displacement in a graduated beaker. The framework community was then sorted into the following functional groups (Fig. 2a): (1) mobile macrofauna, including detritivores and/or predators, (2) sessile epilithic macrofauna, encompassing mostly suspension-feeders, and (3) the remaining 'cryptic (hidden) community'. The cryptic community comprises of all biota, that are too small or interwoven with the framework matrix to be physically separated, i.e. the epilithic biofilm on the framework surface (e.g. bacteria, fungi, encrusting sponges, hydroids; Henry et al., 2016), and the endolithic community inside the dead framework (e.g. bacteria, fungi, sponges, bryozoans, foraminiferans; Beuck et al., 2010). Macrofauna (1–2) was additionally sorted into broad taxonomic groups (Supplementary Table A.2). All samples (1–3) were stored frozen (−20 °C). For analysis, samples were lyophilized, weighed (dry mass), ground, and homogenized by pestle and mortar (macrofauna) or ball mill (framework with cryptic community). Subsequently, samples were acidified with HCl to remove inorganic carbon (Maier et al., 2019), and analysed for organic carbon content (OC) and carbon isotope composition ($\delta^{13}C$) on an elemental analyser coupled to an isotope ratio mass spectrometer (EA-IRMS, Flash 1112, DELTA-V, THERMO). $\delta^{13}C$ measurements provide the non-enriched background values for the stable isotope tracer feeding experiment (see 2.5.4). It should be noted that the endolithic community (3) cannot be separated from the (dead) intraskeletal organic matrix, which was produced by the corals antemortem and remains after death (Ingalls et al., 2003; Falini et al., 2015). The OC of the endolithic community may hence be overestimated.

### 2.5. Stable isotope tracer feeding experiment

#### 2.5.1. Substrate enrichment

Two $^{13}C$-enriched substrates were prepared prior to the cruise, (1) lyophilized diatoms, as a proxy for 'phytodetritus', and (2) dissolved organic matter (DOM) derived from diatoms. The diatoms (*Skeletonema marinoi*, NIOZ culture collection) were cultured axenically under a 12 h-light 12 h-dark cycle, in 1 L-F/2 culture flasks (7 batches of 12 flasks). For $^{13}C$-enrichment, 2 mM $NaHCO_3$ (99 mol-% $^{13}C$) was added. After three weeks, the diatoms were collected on a 0.45 µm-filter, rinsed with

ca. 1 L of artificial seawater to remove residual medium, and centrifuged (1500 rpm). The diatom pellet was frozen (−20 °C) and lyophilized. One diatom batch was used as $^{13}$C-enriched phytodetritus-substrate. For the extraction of $^{13}$C-enriched DOM, six diatom batches (10 g dry mass) were mixed with ultrapure water to lyse the cells. The lysate was centrifuged (4000 rpm) to remove particulate cell residuals, then subsequently 0.22 μm-filtered (sterile), frozen (−20 °C) and lyophilized. Subsamples of $^{13}$C-enriched phytodetritus and $^{13}$C-enriched DOM were analysed without acidification on the EA-IRMS to determine their fractional abundance of $^{13}$C ($F^{13}_{substrate}$, i.e. $F^{13}_{phytodetritus}$: 32.6%, $F^{13}_{DOM}$: 24.4%). Throughout this manuscript, the term 'tracer-C' signifies the total carbon ($^{13}$C + $^{12}$C) derived from the substrates phytodetritus or DOM.

#### 2.5.2. Framework preparation

Fragments of new and old (dead) framework from the mound flank were combined to form mixed 'framework fragments' (n = 6, Fig. 2b). New framework was carefully attached on top of old framework with a nylon wire to simulate a reef substrate with increasing degradation in deeper layers. Framework fragments were placed separately in 3.36 L-plexiglass chambers with 0.35 μm-filtered reef water and kept in the dark in a thermo-controlled room (8.5 °C; Fig. 2b). To ensure mixing and substrate suspension, a magnetic stirring bar on the chamber floor created a circular flow around the experimental fragment, which was sitting above on a perforated table.

#### 2.5.3. Feeding

After three days of acclimatization, the framework fragments were fed for three consecutive days with either $^{13}$C-enriched phytodetritus or $^{13}$C-enriched DOM (both n = 3) at a daily rate of 0.1 mmol tracer C $L^{-1}$ $d^{-1}$, i.e. in total 1.01 mmol tracer C fragment$^{-1}$ (3 d)$^{-1}$ or 0.04 ± 0.01 mmol tracer C (mmol fragment OC)$^{-1}$ (3 d)$^{-1}$. The food concentration was chosen to be high enough to ensure detectable isotope enrichment of the dead-framework community, while still resembling natural reef concentrations (>0.1 mmol total organic carbon $L^{-1}$; Maier et al., 2011; Van Duyl et al., 2008). The two substrates were fed at the same concentration to ensure comparability. Prior to feeding, the substrates were dissolved/suspended in 40 mL filtered reef water. The DOM solution was again 0.22 μm-filtered to remove potential colloids. The substrate solution/suspension was added to the chambers by syringe (Fig. 2b). Daily feeding lasted for 12 h. Then the water was partially exchanged with fresh 0.35 μm-filtered reef water, while keeping the fragments immersed to limit disturbance. For each substrate, duplicate seawater controls without framework were run to account for planktonic tracer-C respiration (see 2.5.4).

#### 2.5.4. Substrate incorporation and respiration

Two parameters were measured to verify whether the framework community utilized the $^{13}$C-enriched substrates (phytodetritus/DOM), i.e. tracer-C incorporation and tracer-C respiration. Tracer-C incorporation means incorporation of carbon ($^{13}$C+$^{12}$C) from the substrates, and includes food uptake by the framework biota, but also physical substrate retention on the framework surface (mostly relevant for particulate phytodetritus). Tracer-C incorporation is measured as the appearance of $^{13}$C in the dead-framework community (Fig. 2b). Tracer-C respiration means respiration of carbon ($^{13}$C+$^{12}$C) from the substrates. This additional parameter was used to verify that the substrates were not only retained, but also used for community metabolism. Tracer-C respiration is measured as the production of $^{13}$C-enriched dissolved inorganic carbon (DI$^{13}$C, Fig. 2b).

To measure DI$^{13}$C production, the framework fragments were individually incubated in 0.35 μm-filtered reef water for 20–22 h after the last feeding day. Incubations of seawater controls (see 2.5.3) served to measure planktonic DI$^{13}$C production. For the incubation, the chambers were flushed with 0.35 μm-filtered reef water (3.5 L) to remove residual substrate and closed with no air-bubbles. At the start (t0) and end (t1) of the incubation, the water was sampled for DI$^{13}$C. After the t0-sampling, the chamber was refilled with 0.35 μm-filtered reef water. DI$^{13}$C was likewise measured in the refill water. The DI$^{13}$C water samples were filled in 10 mL-headspace vials, closed with no air-bubbles, fixed with 10 μL of a saturated mercury chloride solution and stored at 4 °C. DIC concentration was measured on an Apollo SciTech AS-C3, and DIC-$\delta^{13}$C on an EA-IRMS (see 2.4). A detailed description of analytical procedures and stable isotope calculations can be found in Maier et al. (2020b). In short, DI$^{13}$C concentrations at t0 and t1 (DI$^{13}C_{t0}$, DI$^{13}C_{t1}$) were calculated as DIC concentration · $F^{13}_{DIC}$. $F^{13}_{DIC}$ was derived from $\delta^{13}C_{DIC}$ with the standard Vienna Pee Dee Belemnite (R = 0.0111802). The tracer-C respiration rate was calculated as

$$TracerC-respiration = \frac{(DI^{13}C_{t1} - DI^{13}C_{t0}) - (DI^{13}C_{t1\,control} - DI^{13}C_{t0\,control})}{F^{13}_{substrate} \cdot OC_{framework} \cdot t},$$

where DI$^{13}C_{t1\ control}$ and DI$^{13}C_{t0\ control}$ are the DI$^{13}$C concentrations in the seawater control incubations (Supplementary Table A.6), $F^{13}_{substrate}$ the fractional abundance of $^{13}$C in phytodetritus/DOM (see 2.5.1), $OC_{framework}$ the organic carbon content of the framework, and t the incubation time. The tracer-C respiration rate was extrapolated to three days for comparability with tracer-C incorporation.

To measure tracer-C incorporation after the incubation, the biota of the new and old framework fragments were separately sorted into functional and taxonomic groups (Fig. 2b), as described in 2.4. The remaining cryptic community was additionally separated in (a) 'epilithic biofilm', scraped off the framework surface with a scalpel (microorganisms and small, encrusting fauna), and (b) the remaining 'endolithic community' (fauna and microorganisms inside the framework). The samples were individually analysed for organic carbon content (OC) and $\delta^{13}$C (see 2.4).

The tracer-C incorporation rate in each sample was calculated as

$$TracerC-incorporation = \frac{\left(F^{13}_{sample} - F^{13}_{baseline}\right) \cdot OC_{sample}}{F^{13}_{substrate}}$$

where $F^{13}$ is the fractional abundance of $^{13}$C, in the sample ($F^{13}_{sample}$), in the non-enriched background samples ($F^{13}_{baseline}$ = 0.0108, see 2.4), and in the substrates ($F^{13}_{substrate}$, see 2.5.1). $OC_{sample}$ is the sample organic carbon content. The tracer-C incorporation rate refers to three days feeding time. $F^{13}$ is calculated from $\delta^{13}$C as explained in Maier et al. (2019). Tracer-C incorporation into individual samples were summed to determine the tracer-C incorporation into (a) the entire framework fragment (old versus new), (b) the different functional groups and (c) the different macrofauna taxa (Fig. 2b). Tracer-C incorporation rates were standardized to organic carbon content (μmol tracer-C (mmol OC)$^{-1}$ (3 d)$^{-1}$). For comparability between studies, rates standardized to grams dry mass are reported in Supplementary Table A.6.

### 2.6. Data analysis

All data presented in this paper are available at http://doi.org/10.5281/zenodo.4076147 and as 'Supplementary Tables'. Data in text are reported as mean ± standard deviation. Computations and analyses were done in R 4.4.0 (R Core Team, 2020).

#### 2.6.1. Cross-mound video transect

Benthic cover of (a) live corals, (b) new (dead) framework, (c) old (dead) framework, (d) sediment plus coral rubble, (e) sponges and (f) other macro- and megafauna was plotted along the cross-mound transect. To identify the correlation between the benthic cover of habitat or fauna variables (a-f), a Pearson correlation matrix was calculated with the R package 'corrplot' (Wei and Simko, 2017).

#### 2.6.2. Incubation experiment and framework community composition

We compared the community composition between new and old

(dead) framework (see 2.4, Fig. 2a) for (1) total community organic carbon content (in OC per gram dry mass), (2) composition of functional groups (as percentage OC in 'cryptic' community, sessile epilithic macrofauna, mobile macrofauna), and (3) composition of macrofauna taxa (in percentage OC). Furthermore, we compared $O_2$, DIN and DOC fluxes (benthic fluxes) between old and new framework.

#### 2.6.3. Stable isotope tracer feeding experiment

We compared the tracer-C incorporation (see 2.5.4) from phytodetritus with the tracer-C incorporation from DOM between (1) new and old (dead) framework, (2) the functional groups and (3) the macrofauna taxa. Here, OC-specific tracer-C incorporation rates (in µmol tracer-C (mmol OC)$^{-1}$ (3 d)$^{-1}$) were interpreted as the efficiency by which the respective organisms incorporated a substrate. In addition, we used the relative tracer-C incorporation into different functional groups and taxa (in percent of totally incorporated tracer-C) to identify dominant carbon sinks in the community.

## 3. Results

### 3.1. Cross-mound video transect

The video transect over Haas Mound started at the southern side at 670 m water depth (Fig. 3a). The southern flank increases steeply until the peak at 540 m water depth. At the northern side behind the peak, the topography descends steeply for 20 m. The steep zones flanking the peak at the south and north are called 'summit area' here. Behind the summit area, the northern flank continues into a 700 m-wide slightly-sloping plateau (560–590 m water depth). Behind the plateau, the mound descends steeply (northern flank) until the end of the transect at 650 m water depth.

Dead framework (new plus old) covered on average 64% ± 29% of the transect (Fig. 3b). New dead framework could be clearly distinguished from old dead framework in the video stills due to its brighter colour (Fig. 1b, Supplementary Figure A.1). Old dead framework dominated the reef, covering 50% ± 24% of the transect, while new dead framework covered 14% ± 11%, live corals 8% ± 12% and sediment plus coral rubble 16% ± 21%.

Benthic cover of live corals, new and old dead framework, sediment and sponges was heterogeneous along the transect (Fig. 3b). Live coral colonies occurred mostly in the summit area, where they formed ridges perpendicular to the slope; only here, their average cover (over 21 transect positions) exceeded 10%. The live coral zone likewise showed a high benthic cover of new and old dead framework. The plateau was covered mostly by old dead framework and sediment plus coral rubble, which was abundantly colonized by large erect hexactinellid sponges of the species *Nodastrella nodastrella* (formerly *Rossella nodastrella*). The deeper, steeper section of the northern flank showed another smaller local maximum of live corals, new and old dead framework. At the deepest points of the transect (start and end), sediment plus coral rubble dominated.

New dead framework was positively correlated with live corals (Table 1). Old dead framework was positively correlated with new dead framework, but not with live corals. Sediment was negatively correlated with live corals, new and old dead framework. Sponges (mostly *Nodastrella nodastrella*) were negatively correlated with live corals. The sum of other macro- and megafauna was positively correlated with new dead framework.

### 3.2. Dead-framework community composition

Old dead framework collected from the mound summit had the

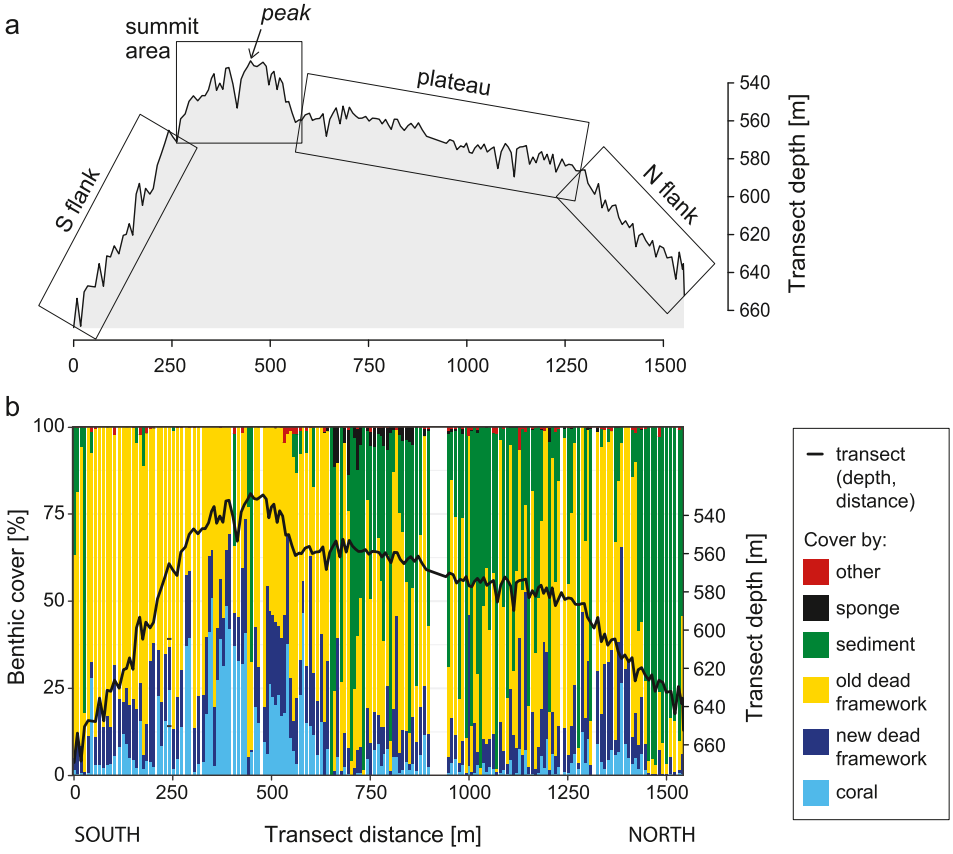


**Fig. 3.** South-to-north video transect across Haas Mound. (a) Transect depth profile and 'zones'. (b) Benthic cover (in %) of live reef-building corals ('coral'), new and old dead framework, sediment plus coral rubble ('sediment'), erect sponges ('sponge') and other macro- or megafauna ('other'); black line: transect depth profile.

**Table 1**
Correlation between benthic cover of sediment, sponges (*Nodastrella nodastrella*), live reef-building corals ('coral'), new and old dead framework, and other macro-and megafauna ('other fauna') on the Haas Mound video transect. R: Pearson correlation coefficient, p: significance of correlation.

| | sediment | | sponge | | coral | | new dead framework | | old dead framework | | other fauna | |
|---|---|---|---|---|---|---|---|---|---|---|---|---|
| | r | p | r | p | r | p | r | p | r | p | r | p |
| **sediment** | 1.00 | 0.00 | | | | | | | | | | |
| **sponge** | 0.11 | 0.17 | 1.00 | 0.00 | | | | | | | | |
| **coral** | -0.47 | 0.00 | -0.17 | 0.03 | 1.00 | 0.00 | | | | | | |
| **new dead framework** | -0.69 | 0.00 | -0.12 | 0.12 | 0.35 | 0.00 | 1.00 | 0.00 | | | | |
| **old dead framework** | -0.85 | 0.00 | -0.10 | 0.21 | 0.02 | 0.76 | 0.34 | 0.00 | 1.00 | 0.00 | | |
| **other fauna** | -0.12 | 0.11 | -0.07 | 0.38 | 0.02 | 0.81 | 0.22 | 0.00 | 0.03 | 0.67 | 1.00 | 0.00 |

highest total-community organic carbon content (OC: 0.21 ± 0.02 mmol OC (g DM)$^{-1}$). The average OC of new and old dead framework from the flank was similar (0.15 ± 0.01 and 0.11 ± 0.05 mmol OC (g DM)$^{-1}$, respectively), with a higher variability in the old dead framework.

Old dead framework was strongly dominated by a cryptic ('hidden') community (Fig. 4a, endolithic community plus epilithic biofilm), which contributed over 90% to the total-community OC. It should be noted that this OC pool includes the live biomass of the framework community, but also the dead intraskeletal organic matrix. Macrofauna (sessile and mobile) only formed 7% and 4% of the total-community OC. On the new dead framework, macrofauna formed a substantial part of the community OC (sessile: 22%, mobile: 12%), but the cryptic community still comprised the largest OC share (66%). Dominant macrofauna taxa on the new framework (in terms of OC, Fig. 4b) included the sessile suspension feeders *Protanthea simplex* (sea anemone, order Actiniaria), Stylasteridae (class Hydrozoa), *Asperarca nodulosa* (class Bivalvia), emergent sponges (phylum Porifera), and mobile macrofauna from the families Ophiuroidea (brittle stars, phylum Echinodermata) and Hesionidae (class Polychaeta). Macrofauna taxa dominating the old framework (in terms of OC) were *Asperarca nodulosa* in the flank- and summit-samples, Actiniaria and the tube-forming polychaete *Eunice* sp. in the flank-sample, and emergent sponges (Porifera) and the tube-forming suspension-feeding polychaete *Chaetopterus* sp. in the summit-sample.

### 3.3. Fluxes of oxygen, dissolved organic carbon and dissolved inorganic nitrogen

The oxygen consumption of the dead framework ranged from 0.078 to 0.182 µmol $O_2$ (mmol OC)$^{-1}$ h$^{-1}$ (Fig. 5a; dry-mass and volume-specific oxygen consumption rates are provided as Supplementary Table A.1).

Fluxes of dissolved inorganic nitrogen (DIN) differed between new and old dead framework. The new framework released ammonium (0.005 ± 0.001 µmol $NH_4^+$ (mmol OC)$^{-1}$ h$^{-1}$), while nitrate fluxes were highly variable (Fig. 5c and d). The old framework released only nitrate (flank-sample: 0.016 ± 0.005 µmol $NO_3^-$ (mmol OC)$^{-1}$ h$^{-1}$, summit-sample: 0.014 ± 0.002 µmol $NO_3^-$ (mmol OC)$^{-1}$ h$^{-1}$).

New and old dead framework took up natural dissolved organic carbon (DOC) at ambient reef concentrations; the incubation water collected 10 m above the reef naturally contained 66 µmol DOC L$^{-1}$ (Supplementary Table A.5, t0 start concentrations). DOC uptake rates ranged between 0.005 and 0.122 µmol C (mmol OC)$^{-1}$ h$^{-1}$, with no clear differences between new and old dead framework (Fig. 5b). DOC uptake represented on average 29% of the aerobic carbon respiration (assuming an $O_2$:$CO_2$ ratio of 1:1, Glud et al., 2008).

### 3.4. Utilization of DOM versus phytodetritus

In the stable isotope tracer feeding experiment, the dead-framework community utilized both substrates, DOM and phytodetritus. DOM and phytodetritus were incorporated at similar rates (DOM: 4.8 ± 0.6 µmol C (mmol OC)$^{-1}$ (3 d)$^{-1}$, phytodetritus: 6.3 ± 0.5 µmol C (mmol OC)$^{-1}$ (3 d)$^{-1}$). The old dead framework showed slightly higher tracer-C incorporation rates for both substrates compared to the new dead framework (Fig. 6a). Tracer-C from DOM and phytodetritus was also respired (DOM: 0.3 ± 0.2 µmol C (mmol OC)$^{-1}$ (3 d)$^{-1}$; phytodetritus: 2.1 ± 0.4

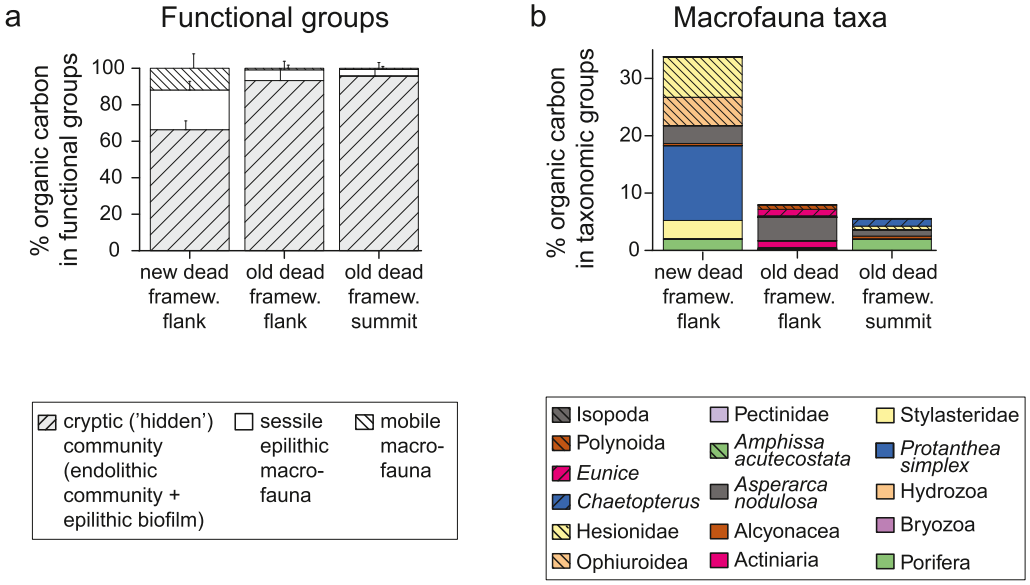


**Fig. 4.** Dead-framework community composition. Comparison between new and old dead framework ('framew.') from mound flank and summit (summit box core did not contain new framework). (a) Percent of the total-community organic carbon in indicated functional groups. Error bars indicate standard deviations. (b) Percent of the total-community organic carbon in indicated macrofauna taxa.

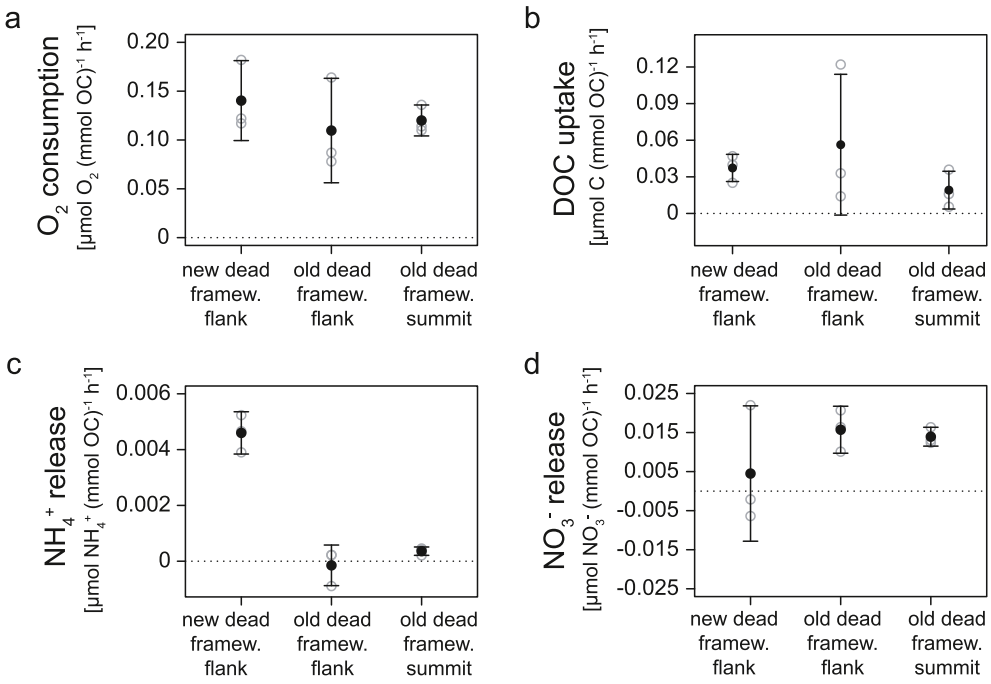


**Fig. 5.** Oxygen and nutrient fluxes of new dead framework ('framew.') from the mound flank, old dead framework from the mound flank and summit. Rates of (a) oxygen consumption, (b) dissolved organic carbon uptake, (c) ammonium release, and (d) nitrate release per mmol organic carbon (OC). Error bars indicate standard deviations.

µmol C (mmol OC)$^{-1}$ (3 d)$^{-1}$), confirming substrate metabolization.

The epilithic biofilm showed the highest phytodetritus incorporation rate of all functional groups (Fig. 6b). This effect was more pronounced on the old dead framework than on the new dead framework. DOM incorporation into the epilithic biofilm was lower compared to phytodetritus incorporation. The endolithic community showed the second-highest rates of phytodetritus and DOM incorporation, with no substantial difference between the substrates. Sessile epilithic macrofauna (mostly suspension-feeders) and mobile macrofauna incorporated phytodetritus and DOM at largely similar rates (Fig. 6b).

On the old dead framework, over 70% of the total incorporated phytodetritus and DOM ended up in the endolithic community, which represented the largest C sink (Table 2). The epilithic biofilm retained another 20% of the substrates, followed by the sessile and mobile macrofauna (together <10%). On the new dead framework, the endolithic community was less abundant (in terms of OC), and accordingly retained only around 50% of the phytodetritus and DOM, followed by the sessile epilithic macrofauna (>30%), the epilithic biofilm (>10%) and the mobile macrofauna (<10%).

All present macrofauna taxa incorporated DOM and phytodetritus (Fig. 6c) at rates between 0.5 and 22.2 µmol C (mmol OC)$^{-1}$ (3 d)$^{-1}$. Several taxa incorporated DOM and phytodetritus at similar rates; these included emergent sponges (Porifera), Hydrozoa, the anemone *Protanthea simplex* and the suspension-feeding polychaete *Chaetopterus* sp. Those taxa likewise displayed the highest DOM incorporation rates. The taxa Stylasteridae, Alcyonacea, *Asperarca nodulosa* and Ophiuroidea incorporated phytodetritus at higher rates than DOM. Stylasteridae displayed the highest phytodetritus incorporation rate, closely followed by Porifera, Hydrozoa, *Protanthea simplex* and Ophiuroidea. The most abundant macrofauna taxa (in terms of OC), i.e. Stylasteridae and the anemone *Protanthea simplex*, represented the largest C sinks within the macrofauna community (Table 2).

## 4. Discussion

The data presented here suggest that the 'dead' cold-water coral (CWC) framework boosts the metabolic activity of CWC reefs, by enhancing resource retention and recycling in a 'filtration-recycling factory' (Fig. 7). We found that on Haas Mound (Logachev CWC province), dead framework forms the most abundant habitat and hosts a diverse community of sessile suspension-feeding macrofauna, mobile macrofauna and cryptic organisms 'hidden' in the dead-framework matrix. Our data indicate that the dead-framework community contributes substantially to the metabolic activity of the CWC reef. We show that the dead framework filters phytodetritus particles in two ways, i.e. through (1) active, biological filtration by suspension-feeders and (2) passive, physical retention on the 'sticky' biofilm-covered surface. Further, our data indicate that the diverse faunal-microbial community of the dead framework recycles 'waste' materials, such as dissolved organic matter (DOM) and dissolved inorganic nitrogen (DIN). In the following, we discuss the important role of the dead framework on CWC reefs.

### 4.1. Abundance and distribution of dead framework

The high abundance of dead framework, that we observed all over Haas Mound, is characteristic of CWC reefs (Wilson, 1979; Freiwald and Wilson 1998; Vad et al., 2017). While live corals are particularly abundant at the mound summit, their dead framework dominates the sloping mound flanks (Fig. 3). This zonation pattern is typical of CWC mounds (De Haas et al., 2009; Lim et al., 2017; Conti et al., 2019) and reefs (Freiwald et al., 2002). On the mound summit, live corals find favourable feeding and growth conditions due to the locally increased vertical transport of phytodetritus from the ocean surface (White et al., 2005; Mohn et al., 2014; Soetaert et al., 2016). The increased vertical transport is caused by the large mound structures, that partially block the tidal current and induce tidal pumping, turbulence (Van Haren et al., 2014; Cyr et al., 2016; Juva et al., 2020) and 'downwelling' of surface water (White et al., 2005; Mohn et al., 2014; Soetaert et al., 2016). On the flanks, conditions for live corals are less suitable, probably because downwelling intensity is lower (Mohn et al., 2014; Cyr et al., 2016; Soetaert et al., 2016) and phytodetritus is already depleted by the filtering reef community on the summit (Lavaleye et al.,

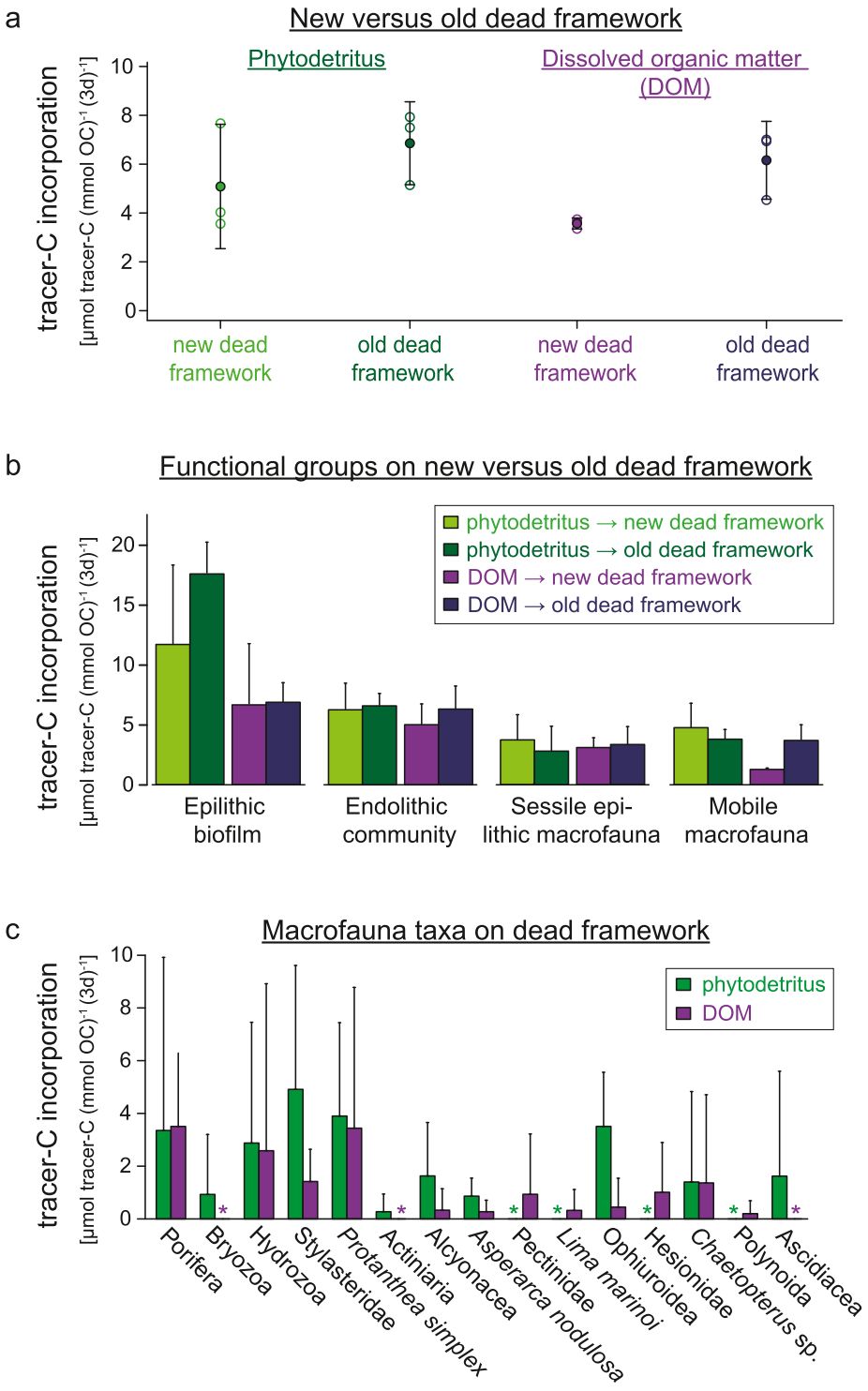


**Fig. 6.** Incorporation of phytodetritus (in green) versus dissolved organic matter (DOM, in purple) by the dead-framework community; measured as tracer-C incorporation, i.e. incorporation of carbon ($^{13+12}$C) from phytodetritus or DOM per mmol organic carbon (OC) per three days (3d) of feeding time. (a) Tracer-C incorporation into new versus old dead framework. (b) Tracer-C incorporation into the indicated functional groups on new versus old dead framework. (c) Tracer-C incorporation into the indicated macrofauna taxa; * taxon not present in this feeding treatment. Error bars indicate standard deviations. (For interpretation of the references to colour in this figure legend, the reader is referred to the Web version of this article.)

2009; Wagner et al., 2011). Here, dead framework contributes substantially to mound development (Mienis et al., 2009b), as it traps suspended sediment and prevents erosion of loose sediment particles (De Haas et al., 2009; Mienis et al., 2019). On the mound plateau, near-absence of live corals and dominance of old dead framework, small coral rubble and large sediment patches (Fig. 3, Supplementary Figure A.1b) signify advanced framework erosion. The disintegrated framework has a reduced capacity to trap suspended particles and strong currents wash away formerly deposited sediment, eroding the mound structure (De Haas et al., 2009; Mienis et al., 2009b). Haas Mound thus appears to exert a positive feedback on mound growth at the coral-covered summit and dead-framework covered flanks and a negative feedback at the plateau, an example of scale-dependent self-organization (Van der Kaaden et al., 2020).

### 4.2. Dead-framework community composition

The diverse community associated with the dead framework (Fig. 4) contributes substantially to total reef diversity (Mortensen et al., 1995; Henry and Roberts, 2007). The differential communities that we found on new versus old dead framework likely relate to progressive substrate

**Table 2**
Sinks of phytodetritus and dissolved organic matter (DOM) in the dead-framework community, as relative tracer-C incorporation from phytodetritus or DOM into different functional groups (upper table) and macrofauna taxa (lower table). Data are shown separately for new and old dead framework.

Relative tracer-C incorporation into functional groups [% of totally incorporated tracer-C]

| | Phytodetritus | | Dissolved organic matter | |
|---|---|---|---|---|
| | new dead framework | old dead framework | new dead framework | old dead framework |
| Epilithic biofilm | 12 | 20 | 12 | 22 |
| Endolithic community | **53** | **73** | **49** | **75** |
| Sessile epilithic macrofauna | 34 | 6 | 36 | 2 |
| Mobile macrofauna | 1 | 2 | 4 | 1 |

**Relative tracer-C incorporation into macrofauna taxa [% of totally incorporated tracer-C]**

| | Phytodetritus | | Dissolved organic matter | |
|---|---|---|---|---|
| | new dead framework | old dead framework | new dead framework | old dead framework |
| Porifera | 2 | 1 | 0 | 2 |
| Bryozoa | 0 | 0 | 0 | 0 |
| Hydrozoa | 0 | 1 | 0 | 0 |
| Stylasteridae | **26** | 0 | **19** | 0 |
| *Protanthea simplex* | 4 | 1 | **13** | 0 |
| Actiniaria | 0 | 0 | 0 | 0 |
| Alcyonacea | 1 | 0 | 1 | 0 |
| *Asperarca nodulosa* | 1 | 1 | 0 | 0 |
| Pectinidae | 0 | 0 | 0 | 0 |
| *Lima marinoi* | 0 | 0 | 2 | 0 |
| Ophiuroidea | 1 | 2 | 0 | 0 |
| Hesionidae | 0 | 0 | 3 | 1 |
| *Chaetopterus sp.* | 0 | 2 | 0 | 0 |
| Polynoida | 0 | 0 | 1 | 0 |
| Ascidiacea | 0 | 2 | 0 | 0 |

instability (Beuck and Freiwald, 2005; Mortensen and Fosså, 2006; Hennige et al., 2020). New dead framework is more stable, enabling attachment of sessile and mobile macrofauna, that form around 30% of the community organic carbon (Fig. 4). In contrast, the porous old framework seems to hamper macrofauna attachment on the outer surface ('epilithic') and we only found few specialized macrofauna taxa such as the bivalve *Asperarca nodulosa* (Kazanidis et al., 2016). Instead, the old framework is dominated by a cryptic ('hidden') community (Fig. 4), which is known to consist of microorganisms (bacteria, fungi) and bioeroding fauna, e.g. bryozoans, foraminiferans, and sponges (Beuck and Freiwald, 2005). Since the cryptic community cannot be separated from the dead organic matrix, which the corals produced antemortem (Ingalls et al., 2003; Falini et al., 2015), its OC content was likely overestimated. Nevertheless, the high metabolic activity of old and new dead framework (see following paragraphs) indicates that the OC of the dead organic matrix was low relative to the OC of the live cryptic community. The dominance of old dead framework, that we observed on Haas Mound, implies that the cryptic community strongly dominates the total reef community. A strong dominance of cryptic cavity-dwellers (coelobites) was likewise observed on tropical reefs (Richter et al., 2001) and may be a common trait of calcareous reefs.

### 4.3. Dead framework contribution to reef oxygen consumption

Our study indicates that dead framework plays an important role in the benthic metabolism of CWC reefs. The oxygen consumption rate of the dead-framework community (0.01–0.03 µmol $O_2$ (g $DM_{framework}$)$^{-1}$ $h^{-1}$, at 8.5 °C) is on average ten times lower compared to live corals (*Lophelia pertusa*: 0.1–0.3 µmol $O_2$ (g $DM_{coral}$)$^{-1}$ $h^{-1}$, Khripounoff et al., 2014 at 10 °C; Maier et al., 2019 at 8 °C). Nevertheless, since dead framework covers an eight times larger reef area compared to live corals, it likely contributes at least eight times more to the total framework dry mass (live plus dead). Based on these assumptions, dead framework (DF) and live corals (LC) would contribute almost equally to the total reef oxygen consumption (DF:LC = 8:10). However, since dead framework forms a thick three-dimensional layer on the reef, also below live corals (Freiwald et al., 2002; De Haas et al., 2009; Mienis et al., 2009b), its contribution to total framework dry mass and reef oxygen consumption could even be higher. A previous study estimated that dead framework

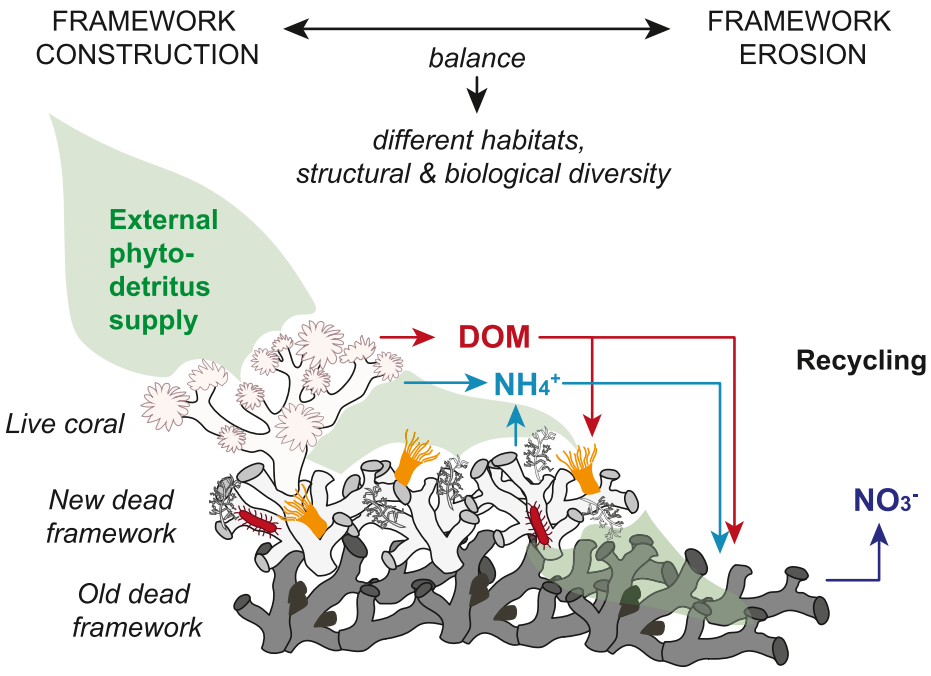


**Fig. 7.** Drivers of resource retention and recycling on cold-water coral reefs, a conceptual model.

contributes 10–75% to the total reef oxygen consumption at the Logachev mounds (De Froe et al., 2019).

### 4.4. Filtration of suspended phytodetritus

The feeding experiment with $^{13}$C-enriched phytodetritus confirmed our initial assumption that the dead framework efficiently traps phytodetritus particles (i.e. POM), which would not settle on a flat sea floor (De Haas et al., 2009; Mienis et al., 2009a; Van Oevelen et al., 2009), through physical and biological filtration. Sediment traps obviously lack these filtration mechanisms, and therefore, underestimate the deposition of phytodetritus on CWC reefs. Efficient particle filtration could hence provide one explanation for the mismatch between the low POM flux measured by sediment traps, and the high metabolic activity (organic matter mineralization) of the deep reefs (Van Oevelen et al., 2009).

Biological particle filtration is driven by suspension-feeders living on or inside the dead framework, indicated by their incorporation of $^{13}$C-enriched phytodetritus (Fig. 6, sessile epilithic macrofauna and endolithic community). This experimental observation is corroborated by the low $\delta^{15}$N value of most reef-associated suspension feeders at Rockall Bank, which indicates feeding on fresh phytodetritus (Duineveld et al., 2007). Efficient biological filtration is also known from reef framework cavities on tropical reefs, where encrusting filter-feeders remove large amounts of phytoplankton (Richter et al., 2001). Interestingly, the cryptic community hidden on the surface and inside the framework branches forms the largest phytodetritus sink (Table 2). This corroborates results from a Rockall Bank food web model (Van Oevelen et al., 2009), which show that microbes, thinly encrusting and endolithic fauna (e.g. sponges) are the dominant carbon consumers on a CWC reef.

Physical particle filtration is suggested by the high phytodetritus incorporation in the epilithic, surface-covering biofilm of the framework (Fig. 6b). Biofilms efficiently sequester organic and inorganic particles through sorption (Flemming et al., 2016) and facilitate detritus trapping on dead CWC framework (Freiwald and Wilson, 1998). Physical filtration is facilitated by the branched framework structure which reduces the local current velocity (De Haas et al., 2009; Mienis et al., 2009a) and induces turbulence (Mienis et al., 2019). Increased framework degradation appears to stimulate the adhesion effect (Fig. 6b; Freiwald and Wilson, 1998), likely because increased porosity (Hennige et al., 2020) facilitates biofilm development (Beuck and Freiwald, 2005). Physically-retained phytodetritus, in turn, seems to provide an important food source for mobile detritivore macrofauna (Fig. 6b; Duineveld et al., 2007; Henry et al., 2013).

With the effective combination of physical and biological filtration, a CWC reef acts as a huge filter that removes organic particles from the overlaying water (see also Wagner et al., 2011). The 'reef filter' may provide a number of important deep-sea ecosystem services, such as sustenance of complex food webs (Van Oevelen et al., 2009), engineering of a 'topographically-enhanced carbon pump' (Soetaert et al., 2016), and organic carbon sequestration to the deep sea. Deep-sea CWC reefs could therefore play a 'paramount role' in the marine carbon cycle, just like shallow-water suspension-feeding communities (Gili and Coma, 1998; Rossi and Bramanti, 2020).

### 4.5. DOM recycling

The presented data likewise confirm our second assumption that the dead framework efficiently (re)cycles material, i.e. DOM and DIN. We provide the first evidence of 'natural' DOC uptake, i.e. at ambient reef concentration (66 μM DOC) and composition (Fig. 5b). High rates of DOC uptake in relation to oxygen consumption (respiration) suggest that DOC is an important food source to fuel the metabolism of the framework community. On the reef, DOC is produced by the corals as mucus (Wild et al., 2008) and DOC uptake is considered an important recycling pathway (Rix et al., 2016). Previously, benthic DOM uptake on coral reefs was attributed mostly to sponges, aided by their symbiotic microbiome (Reiswig, 1981; Yahel et al., 2003; Ribes et al., 2012). However, our additional feeding experiment with $^{13}$C-enriched DOM demonstrates that recycling is mediated by the entire framework community. All functional groups and macrofauna taxa incorporated DOM, mostly at similar rates as phytodetritus (Fig. 6). Lower DOM incorporation into the epilithic biofilm likely relates to the dissolved nature of the substrate, which, unlike phytodetritus, is not physically retained.

Most DOM is retained in the (endolithic) cryptic community hidden inside the dead-framework branches (Table 2). Likewise in tropical reef cavities, the cryptic community shows high DOM uptake rates (De Goeij and van Duyl, 2007). Microorganisms, that form an abundant part of the endolithic community (Beuck and Freiwald, 2005; Van Bleijswijk et al., 2015), might hence play an important quantitative role in DOM recycling on CWC reefs. Nevertheless, comparatively high rates of DOM incorporation by macrofauna (Fig. 6) disagree with the previous perception that DOM utilization by animals is negligible (Siebers, 1982). We show that also suspension feeders without abundant microbiomes, such as hydrozoans and the anemone *Protanthea simplex*, incorporate DOM at high rates (Fig. 6), indicating DOM uptake by the animal itself (Wright and Manahan, 1989). Accordingly, a recent study demonstrated that CWC reef bivalves and low-microbial-abundance sponges incorporate DOM at similar rates as high-microbial abundance sponges (Maier et al., 2020b). Furthermore, Rix et al. (2020) demonstrated direct DOM uptake by the sponge host cells.

CWC reef sponges and bivalves release part of the assimilated DOM as a particulate waste product, which in turn feeds the detritivore food chain (Rix et al., 2016; Maier et al., 2020b). Given the ubiquitous utilization of DOM by the framework community, this recycling pathway termed 'sponge loop' (De Goeij et al., 2013) might also be performed by macrofauna taxa other than sponges. DOM recycling may counteract the seasonal limitation of particulate food (Duineveld et al., 2004; Maier et al., 2020a) and sustain the high metabolic activity and complex food web of CWC reefs.

### 4.6. Complex nitrogen cycling

The dead framework demonstrates complex nitrogen cycling, with differential nitrogen release depending on the state of degradation (Fig. 5c and d). New dead framework releases ammonium, at similar OC-specific rates as *Lophelia pertusa* (Khripounoff et al., 2014; Maier et al., 2019). Ammonium is produced by ammonotelic (ammonium-excreting) macrofauna (Wright, 1995), that are relatively abundant on the new framework (Fig. 4). In contrast, net nitrate release by the old dead framework hints at active nitrifying bacteria, which oxidize ammonium to nitrate (reviewed by Stief, 2013). Indeed, nitrifying Bacteria (ammonia oxidizers: *Nitrosomonas*, *Nitrosococcus*; nitrite oxidizers: *Nitrospira*) and Archaea (Thaumarchaeota) occur in the dead framework (endolithic and epilithic, Van Bleijswijk et al., 2015) and as symbionts in reef sponges (Cardoso et al., 2013). Ammonium concentration in ambient reef water is, however, low (Supplementary Table A.5, t0-values) and nitrification of background ammonium cannot explain the high nitrate release (Fig. 5). We therefore suggest that, on the old framework, microbial nitrifiers recycle ammonium, which was previously released by ammonotelic fauna (Fig. 4; Beuck and Freiwald, 2005). Ammonium production by benthic fauna is known to boost microbial nitrogen cycling (Stief, 2013), e.g. in tropical coral reef framework cavities (Risk and Muller, 1983; Rasheed et al., 2002; Van Duyl et al., 2006). The produced nitrate could in turn be used by denitrifying bacterial communities associated with live CWCs (Middelburg et al., 2015) and dead framework (Van Bleijswijk et al., 2015) for the oxidation of organic matter under (temporally) anoxic or suboxic conditions (Hanz et al., 2019; Hebbeln et al., 2020). The suggested exchange of inorganic nitrogen compounds between microbes and fauna on the dead framework could hence stimulate nitrogen recycling within the reef community, similar to tropical coral reefs (Crossland et al., 1991;

Hatcher, 1997).

### 4.7. Conclusion and perspectives

We conclude that the dead CWC framework acts as a 'filtration-recycling factory' (Fig. 7), attributable to its structural complexity and the close interaction between suspension-feeding animals and microbial communities (Fig. 4; Mortensen et al., 1995; Henry and Roberts, 2007; Van Bleijswijk et al., 2015). Enhanced resource retention and recycling on the abundant dead framework provides a missing link to the previously described paradox, i.e. the high metabolic activity of CWC reefs under limited organic matter flux (Van Oevelen et al., 2009). The dead coral framework is, however, under particular threat of ocean acidification, which rapidly and drastically increases the porosity of non-protected coral skeleton (Hennige et al., 2020). Ocean acidification furthermore increases bioerosion (Wisshak et al., 2014), disrupting the balance between reef construction and erosion (Büscher et al., 2019). CWC reefs that already occur below aragonite saturation show little to no dead framework and represent live-CWC 'crusts' rather than structurally-complex reefs (Hennige et al., 2020). Based on the results presented here, those CWC 'crusts' likely have a much lower diversity, metabolic activity, filtration and recycling capacity and presumably a completely different ecosystem function compared to healthy reef 'filtration-recycling factories'. We urgently need to understand the effects of the 'coralporosis' (Hennige et al., 2020) on reef functioning and identify 'climate refuges' (Morato et al., 2020), where functioning CWC reefs can prevail in the future.

## Declaration of competing interest

The authors declare that they have no known competing financial interests or personal relationships that could have appeared to influence the work reported in this paper.

## Acknowledgements

We are grateful to the ship's crew of the *RV Pelagia* and to Pieter van Rijswijk for their support in logistics and sampling and to Gert-Jan Reichart for leading the expedition. We would like to thank the analytical lab of the NIOZ, especially Peter van Breugel, for assistance in organic carbon and isotope analysis and Jan Peene, for dissolved inorganic nitrogen analysis. Further, we are grateful to Claudia Burau (AWI) for dissolved organic carbon analysis. Funding was provided by the Netherlands Organisation for Scientific Research (VIDI grant 864.13.007 to Dick van Oevelen and NWO-VENI grant 863.11.012 to Furu Mienis), by the European Union's Seventh Framework Programme (grant agreement no. 213144, CoralFISH) and the European Union's Horizon 2020 Research and Innovation Programme (grant agreement no. 678760, ATLAS). Ship time was provided by the NIOZ Royal Netherlands Institute for Sea Research.

## Appendix A. Supplementary data

Supplementary data to this article can be found online at https://doi.org/10.1016/j.dsr.2021.103574.

## Data availability

All data presented in this paper are available at 10.5281/zenodo.*4076147 (link will be activated after manuscript acceptance)* and as 'Supplementary Tables'.

## References

Addamo, A.M., Vertino, A., Stolarski, J., García-Jiménez, R., Taviani, M., Machordom, A., 2016. Merging scleractinian genera: the overwhelming genetic similarity between solitary *Desmophyllum* and colonial *Lophelia*. BMC Evol. Biol. 16, 108. https://doi.org/10.1186/s12862-016-0654-8.

Beuck, L., Freiwald, A., 2005. Bioerosion Patterns in a Deep-Water Lophelia Pertusa (Scleractinia) Thicket (Propeller Mound, Northern Porcupine Seabight). In: Freiwald, A., Roberts, J.M. (Eds.), Cold-water Corals and Ecosystems, Erlangen Earth Conference Series. Springer, Berlin, Heidelberg, pp. 915–936. https://doi.org/10.1007/3-540-27673-4_47.

Beuck, L., Freiwald, A., Taviani, M., 2010. Spatiotemporal bioerosion patterns in deep-water scleractinians from off santa maria di Leuca (apulia, ionian sea). Deep-Sea Res. Pt. II 57, 458–470. https://doi.org/10.1016/j.dsr2.2009.08.019.

Büscher, J.V., Wisshak, M., Form, A.U., Titschack, J., Nachtigall, K., Riebesell, U., 2019. In situ growth and bioerosion rates of *Lophelia pertusa* in a Norwegian fjord and open shelf cold-water coral habitat. PeerJ 7, e7586. https://doi.org/10.7717/peerj.7586.

Cardoso, J.F.M.F., van Bleijswijk, J.D.L., Witte, H., Duyl, F.C. van, 2013. Diversity and abundance of ammonia-oxidizing Archaea and Bacteria in tropical and cold-water coral reef sponges. Aquat. Microb. Ecol. 68, 215–230. https://doi.org/10.3354/ame01610.

Cathalot, C., van Oevelen, D., Cox, T.J.S., Kutti, T., Lavaleye, M., Duineveld, G., Meysman, F.J.R., 2015. Cold-water coral reefs and adjacent sponge grounds: hotspots of benthic respiration and organic carbon cycling in the deep sea. Front. Mar. Sci. 2, 1–12. https://doi.org/10.3389/fmars.2015.00037.

Conti, L.A., Lim, A., Wheeler, A.J., 2019. High resolution mapping of a cold water coral mound. Sci. Rep. 9, 1016. https://doi.org/10.1038/s41598-018-37725-x.

Crossland, C.J., Hatcher, B.G., Smith, S.V., 1991. Role of coral reefs in global ocean production. Coral Reefs 10, 55–64. https://doi.org/10.1007/BF00571824.

Cyr, F., van Haren, H., Mienis, F., Duineveld, G., Bourgault, D., 2016. On the influence of cold-water coral mound size on flow hydrodynamics, and vice versa. Geophys. Res. Lett. 43, 775–783. https://doi.org/10.1002/2015GL067038.

De Froe, E., Rovelli, L., Glud, R.N., Maier, S.R., Duineveld, G., Mienis, F., Lavaleye, M., van Oevelen, D., 2019. Benthic oxygen and nitrogen exchange on a cold-water coral reef in the North-East Atlantic Ocean. Front. Mar. Sci. 6 https://doi.org/10.3389/fmars.2019.00665.

De Goeij, J.M., van Duyl, F.C., 2007. Coral cavities are sinks of dissolved organic carbon (DOC). Limnol. Oceanogr. 52, 2608–2617. https://doi.org/10.4319/lo.2007.52.6.2608.

De Goeij, J.M., van Oevelen, D., Vermeij, M.J.A., Osinga, R., Middelburg, J.J., de Goeij, A.F.P.M., Admiraal, W., 2013. Surviving in a marine desert: the sponge loop retains resources within coral reefs. Science 342, 108–110. https://doi.org/10.1126/science.1241981.

De Haas, H., Mienis, F., Frank, N., Richter, T.O., Steinacher, R., de Stigter, H., van der Land, C., van Weering, T.C.E., 2009. Morphology and sedimentology of (clustered) cold-water coral mounds at the south Rockall Trough margins, NE Atlantic Ocean. Facies 55, 1–26. https://doi.org/10.1007/s10347-008-0157-1.

Duineveld, G.C.A., Lavaleye, M.S.S., Berghuis, E.M., 2004. Particle flux and food supply to a seamount cold-water coral community (Galicia Bank, NW Spain). Mar. Ecol. Prog. Ser. 277, 13–23. https://doi.org/10.3354/meps277013.

Duineveld, G.C.A., Lavaleye, M.S.S., Bergman, M.J.N., de Stigter, H., Mienis, F., 2007. Trophic structure of a cold-water coral mound community (Rockall Bank, NE Atlantic) in relation to the near-bottom particle supply and current regime. Bull. Mar. Sci. 81, 449–467.

Falini, G., Fermani, S., Goffredo, S., 2015. Coral biomineralization: a focus on intra-skeletal organic matrix and calcification. Seminars in Cell & Developmental Biology, Biomineralisation & Motorisation of pathogens 46, 17–26. https://doi.org/10.1016/j.semcdb.2015.09.005.

Flemming, H.-C., Wingender, J., Szewzyk, U., Steinberg, P., Rice, S.A., Kjelleberg, S., 2016. Biofilms: an emergent form of bacterial life. Nat. Rev. Microbiol. 14, 563–575. https://doi.org/10.1038/nrmicro.2016.94.

Freiwald, A., Fosså, J.H., Grehan, A., Koslow, T., Roberts, J.M., 2004. Cold-water Coral Reefs. UNEP-WCMC), Cambridge, UK.

Freiwald, A., Hühnerbach, V., Lindberg, B., Wilson, J.B., Campbell, J., 2002. The Sula reef complex, Norwegian shelf. Facies 47, 179–200. https://doi.org/10.1007/BF02667712.

Freiwald, A., Wilson, J.B., 1998. Taphonomy of modern deep, cold-temperate water coral reefs. Hist. Biol. 13, 37–52. https://doi.org/10.1080/08912969809386571.

Gili, J.-M., Coma, R., 1998. Benthic suspension feeders: their paramount role in littoral marine food webs. Trends Ecol. Evol. 13, 316–321. https://doi.org/10.1016/S0169-5347(98)01365-2.

Glud, R.N., Eyre, B.D., Patten, N., 2008. Biogeochemical responses to mass coral spawning at the Great Barrier Reef: effects on respiration and primary production. Limnol. Oceanogr. 53, 1014–1024. https://doi.org/10.4319/lo.2008.53.3.1014.

Hanz, U., Wienberg, C., Hebbeln, D., Duineveld, G., Lavaleye, M., Juva, K., Dullo, W.-C., Freiwald, A., Tamborrino, L., Reichart, G.-J., Flögel, S., Mienis, F., 2019. Environmental factors influencing benthic communities in the oxygen minimum zones on the Angolan and Namibian margins. Biogeosciences. https://doi.org/10.5194/bg-16-4337-2019.

Hatcher, B.G., 1997. Coral reef ecosystems: how much greater is the whole than the sum of the parts? Coral Reefs 16, S77–S91. https://doi.org/10.1007/s003380050244.

Hebbeln, D., Wienberg, C., Dullo, W.-C., Freiwald, A., Mienis, F., Orejas, C., Titschack, J., 2020. Cold-water coral reefs thriving under hypoxia. Coral Reefs 39, 853–859. https://doi.org/10.1007/s00338-020-01934-6.

Hennige, S.J., Wolfram, U., Wickes, L., Murray, F., Roberts, J.M., Kamenos, N.A., Schofield, S., Groetsch, A., Spiesz, E.M., Aubin-Tam, M.-E., Etnoyer, P.J., 2020. Crumbling reefs and cold-water coral habitat loss in a future ocean: evidence of "coralporosis" as an undicator of habitat integrity. Front. Mar. Sci. 7 https://doi.org/10.3389/fmars.2020.00668.

Henry, L.-A., Navas, J.M., Roberts, M., 2013. Multi-scale interactions between local hydrography, seabed topography, and community assembly on cold-water coral reefs. Biogeosciences 10. https://doi.org/10.5194/bg-10-2737-2013.

Henry, L.-A., Roberts, M.J., 2007. Biodiversity and ecological composition of macrobenthos on cold-water coral mounds and adjacent off-mound habitat in the bathyal Porcupine Seabight, NE Atlantic. Deep-Sea Res. Pt. I 54, 654–672. https://doi.org/10.1016/j.dsr.2007.01.005.

Henry, L.-A., Roberts, M.J., 2016. Global Biodiversity in Cold-Water Coral Reef Ecosystems. In: Rossi, S., Bramanti, L., Gori, A., Orejas Saco del Valle, C. (Eds.), Marine Animal Forests: the Ecology of Benthic Biodiversity Hotspots. Springer International Publishing, Cham, pp. 1–21. https://doi.org/10.1007/978-3-319-17001-5_6-1.

Hijmans, R., Williams, E., Vennes, C., 2015. Geosphere: Spherical Trigonometry. R Package. https://CRAN.R-project.org/package=geosphere.

Hoffmann, F., Radax, R., Woebken, D., Holtappels, M., Lavik, G., Rapp, H.T., Schläppy, M.L., Schleper, C., Kuypers, M.M.M., 2009. Complex nitrogen cycling in the sponge *Geodia barretti*. Environ. Microbiol. 11, 2228–2243. https://doi.org/10.1111/j.1462-2920.2009.01944.x.

Ingalls, A.E., Lee, C., Druffel, E.R.M., 2003. Preservation of organic matter in mound-forming coral skeletons. Geochem. Cosmochim. Acta 67, 2827–2841. https://doi.org/10.1016/S0016-7037(03)00079-6.

Jonsson, L.G., Nilsson, P.G., Floruta, F., Lundälv, T., 2004. Distributional patterns of macro- and megafauna associated with a reef of the cold-water coral *Lophelia pertusa* on the Swedish west coast. Mar. Ecol. Prog. Ser. 284, 163–171. https://doi.org/10.3354/meps284163.

Juva, K., Flögel, S., Karstensen, J., Linke, P., Dullo, W.-C., 2020. Tidal dynamics control on cold-water coral growth: a high-resolution multivariable study on eastern Atlantic cold-water coral sites. Front. Mar. Sci. 7 https://doi.org/10.3389/fmars.2020.00132.

Kazanidis, G., Henry, L.-A., Roberts, J.M., Witte, U.F.M., 2016. Biodiversity of *Spongosorites coralliophaga* (Stephens, 1915) on coral rubble at two contrasting cold-water coral reef settings. Coral Reefs 35, 193–208. https://doi.org/10.1007/s00338-015-1355-2.

Khripounoff, A., Caprais, J.-C., Le Bruchec, J., Rodier, P., Noel, P., Cathalot, C., 2014. Deep cold-water coral ecosystems in the Brittany submarine canyons (Northeast Atlantic): hydrodynamics, particle supply, respiration, and carbon cycling. Limnol. Oceanogr. 59, 87–98. https://doi.org/10.4319/lo.2014.59.01.0087.

Kiriakoulakis, K., Fisher, E., Wolff, G., Freiwald, A., Grehan, A., Roberts, J., 2005. Lipids and Nitrogen Isotopes of Two Deep-Water Corals from the North-East Atlantic: Initial Results and Implications for Their Nutrition. In: Freiwald, A., Roberts, J. (Eds.), Cold-Water Corals and Ecosystems. Springer, Berlin, Heidelberg, pp. 715–729.

Lavaleye, M., Duineveld, G., Lundälv, T., White, M., Guihen, D., Kiriakoulakis, K., Wolff, G.A., 2009. Cold-water corals on the Tisler reef: preliminary observations on the dynamic reef environment. Oceanography 22, 76–84.

Lim, A., Wheeler, A.J., Arnaubec, A., 2017. High-resolution facies zonation within a cold-water coral mound: the case of the Piddington Mound, Porcupine Seabight, NE Atlantic. Mar. Geol. 390, 120–130. https://doi.org/10.1016/j.margeo.2017.06.009.

Maier, C., de Kluijver, A., Agis, M., Brussaard, C.P.D., van Duyl, F.C., Weinbauer, M.G., 2011. Dynamics of nutrients, total organic carbon, prokaryotes and viruses in onboard incubations of cold-water corals. Biogeosciences 8, 2609–2620. https://doi.org/10.5194/bg-8-2609-2011.

Maier, S.R., Bannister, R.J., van Oevelen, D., Kutti, T., 2020a. Seasonal controls on the diet, metabolic activity, tissue reserves and growth of the cold-water coral *Lophelia pertusa*. Coral Reefs 39, 173–187. https://doi.org/10.1007/s00338-019-01886-6.

Maier, S.R., Kutti, T., Bannister, R.J., van Breugel, P., van Rijswijk, P., van Oevelen, D., 2019. Survival under conditions of variable food availability: resource utilization and storage in the cold-water coral *Lophelia pertusa*. Limnol. Oceanogr. 64, 1651–1671. https://doi.org/10.1002/lno.11142.

Maier, S.R., Kutti, T., Bannister, R.J., Fang, J.K.-H., van Breugel, P., van Rijswijk, P., van Oevelen, D., 2020b. Recycling pathways in cold-water coral reefs: use of dissolved organic matter and bacteria by key suspension feeding taxa. Sci. Rep. 10, 9942. https://doi.org/10.1038/s41598-020-66463-2.

Middelburg, J.J., Mueller, C.E., Veuger, B., Larsson, A.I., Form, A., van Oevelen, D., 2015. Discovery of symbiotic nitrogen fixation and chemoautotrophy in cold-water corals. Sci. Rep. 5, 1–9. https://doi.org/10.1038/srep17962, 17962.

Mienis, F., Bouma, T.J., Witbaard, R., van Oevelen, D., Duineveld, G.C.A., 2019. Experimental assessment of the effects of cold-water coral patches on water flow. Mar. Ecol. Prog. Ser. 609, 101–117. https://doi.org/10.3354/meps12815.

Mienis, F., de Stigter, H.C., de Haas, H., van Weering, T.C.E., 2009a. Near-bed particle deposition and resuspension in a cold-water coral mound area at the Southwest Rockall Trough margin, NE Atlantic. Deep-Sea Res. Pt. I 56, 1026–1038. https://doi.org/10.1016/j.dsr.2009.01.006.

Mienis, F., van der Land, C., de Stigter, H.C., van de Vorstenbosch, M., de Haas, H., Richter, T., van Weering, T.C.E., 2009b. Sediment accumulation on a cold-water carbonate mound at the Southwest Rockall Trough margin. Mar. Geol. 265, 40–50. https://doi.org/10.1016/j.margeo.2009.06.014.

Mohn, C., Rengstorf, A., White, M., Duineveld, G., Mienis, F., Soetaert, K., Grehan, A., 2014. Linking benthic hydrodynamics and cold-water coral occurrences: a high-resolution model study at three cold-water coral provinces in the NE Atlantic. Prog. Oceanogr. 122, 92–104. https://doi.org/10.1016/j.pocean.2013.12.003.

Morato, T., González-Irusta, J.-M., Dominguez-Carrió, C., Wei, C.-L., Davies, A., Sweetman, A.K., Taranto, G.H., Beazley, L., García-Alegre, A., Grehan, A., Laffargue, P., Murillo, F.J., Sacau, M., Vaz, S., Kenchington, E., Arnaud-Haond, S., Callery, O., Chimienti, G., Cordes, E., Egilsdottir, H., Freiwald, A., Gasbarro, R., Gutiérrez-Zárate, C., Gianni, M., Gilkinson, K., Hayes, V.E.W., Hebbeln, D., Hedges, K., Henry, L.-A., Johnson, D., Koen-Alonso, M., Lirette, C., Mastrototaro, F., Menot, L., Molodtsova, T., Muñoz, P.D., Orejas, C., Pennino, M.G., Puerta, P., Ragnarsson, S.Á., Ramiro-Sánchez, B., Rice, J., Rivera, J., Roberts, J.M., Ross, S.W., Rueda, J.L., Sampaio, Í., Snelgrove, P., Stirling, D., Treble, M.A., Urra, J., Vad, J., Oevelen, D. van, Watling, L., Walkusz, W., Wienberg, C., Woillez, M., Levin, L.A., Carreiro-Silva, M., 2020. Climate-induced changes in the suitable habitat of cold-water corals and commercially important deep-sea fishes in the North Atlantic. Global Change Biol. 26, 2181–2202. https://doi.org/10.1111/gcb.14996.

Mortensen, P.B., Fosså, J.H., 2006. Species diversity and spatial distribution of invertebrates on deep-water *Lophelia* reefs in Norway. In: Proceedings of 10th International Coral Reef Symposium, pp. 1849–1868.

Mortensen, P.B., Hovland, M., Brattegard, T., Farestveit, R., 1995. Deep water bioherms of the scleractinian coral *Lophelia pertusa* (L.) at 64° n on the Norwegian shelf: structure and associated megafauna. Sarsia 80, 145–158. https://doi.org/10.1080/00364827.1995.10413586.

Mueller, C.E., Larsson, A.I., Veuger, B., Middelburg, J.J., van Oevelen, D., 2014. Opportunistic feeding on various organic food sources by the cold-water coral *Lophelia pertusa*. Biogeosciences 11, 123–133. https://doi.org/10.5194/bg-11-123-2014.

R Core Team, 2017. R: A Language and Environment for Statistical Computing. R Foundation for Statistical Computing, Vienna, Austria. URL. https://www.R-project.org/.

Rasheed, M., Badran, M.I., Richter, C., Huettel, M., 2002. Effect of reef framework and bottom sediment on nutrient enrichment in a coral reef of the Gulf of Aqaba, Red Sea. Mar. Ecol. Prog. Ser. 239, 277–285. https://doi.org/10.3354/meps239277.

Reiswig, H.M., 1981. Partial carbon and energy budgets of the bacteriosponge *Verohgia fistularis* (Porifera: Demospongiae) in Barbados. Mar. Ecol. 2, 273–293. https://doi.org/10.1111/j.1439-0485.1981.tb00271.x.

Ribes, M., Jiménez, E., Yahel, G., López-Sendino, P., Diez, B., Massana, R., Sharp, J.H., Coma, R., 2012. Functional convergence of microbes associated with temperate marine sponges. Environ. Microbiol. 14, 1224–1239. https://doi.org/10.1111/j.1462-2920.2012.02701.x.

Richter, C., Wunsch, M., Rasheed, M., Kötter, I., Badran, M.I., 2001. Endoscopic exploration of Red Sea coral reefs reveals dense populations of cavity-dwelling sponges. Nature 413, 726–730. https://doi.org/10.1038/35099547.

Risk, M.J., Muller, H.R., 1983. Porewater in coral heads: evidence for nutrient regeneration. Limnol. Oceanogr. 28, 1004–1008. https://doi.org/10.4319/lo.1983.28.5.1004.

Rix, L., Naumann, M.S., de Goeij, J.M., Mueller, C.E., Struck, U., Middleburg, J.J., van Duyl, F.C., Al-Horani, F.A., Wild, C., van Oevelen, D., 2016. Coral mucus fuels the sponge loop in warm- and cold-water coral reef ecosystems. Sci. Rep. 6, 1–11. https://doi.org/10.1038/srep18715.

Rix, L., Ribes, M., Coma, R., Jahn, M.T., de Goeij, J.M., van Oevelen, D., Escrig, S., Meibom, A., Hentschel, U., 2020. Heterotrophy in the earliest gut: a single-cell view of heterotrophic carbon and nitrogen assimilation in sponge-microbe symbioses. ISME J. 1–14. https://doi.org/10.1038/s41396-020-0706-3.

Roberts, J.M., Wheeler, A.J., Freiwald, A., 2006. Reefs of the deep: the biology and geology of cold-water coral ecosystems. Science 312, 543–547. https://doi.org/10.1126/science.1119861.

Rossi, S., Bramanti, L. (Eds.), 2020. Perspectives on the Marine Animal Forests of the World. Springer International Publishing, Cham. https://doi.org/10.1007/978-3-030-57054-5.

Siebers, D., 1982. Bacterial-invertebrate interactions in uptake of dissolved organic matter. Integr. Comp. Biol. 22, 723–733. https://doi.org/10.1093/icb/22.3.723.

Soetaert, K., Mohn, C., Rengstorf, A., Grehan, A., van Oevelen, D., 2016. Ecosystem engineering creates a direct nutritional link between 600-m deep cold-water coral mounds and surface productivity. Sci. Rep. 6, 35057. https://doi.org/10.1038/srep35057.

Stief, P., 2013. Stimulation of microbial nitrogen cycling in aquatic ecosystems by benthic macrofauna: mechanisms and environmental implications. Biogeosciences 10, 7829–7846. https://doi.org/10.5194/bg-10-7829-2013.

Vad, J., Orejas, C., Moreno-Navas, J., Findlay, H.S., Roberts, J.M., 2017. Assessing the living and dead proportions of cold-water coral colonies: implications for deep-water Marine Protected Area monitoring in a changing ocean. PeerJ 5, e3705. https://doi.org/10.7717/peerj.3705.

Van Bleijswijk, J.D.L., Whalen, C., Duineveld, G.C.A., Lavaleye, M.S.S., Witte, H.J., Mienis, F., 2015. Microbial assemblages on a cold-water coral mound at the SE Rockall Bank (NE Atlantic): interactions with hydrography and topography. Biogeosciences 12, 4483–4496. https://doi.org/10.5194/bg-12-4483-2015.

Van der Kaaden, A.-S., 2021. AnnavdKaaden/Image annotation: image/video annotation and analysis (version v2). Zenodo. https://doi.org/10.5281/zenodo.4575809.

Van der Kaaden, A.-S., van Oevelen, D., Rietkerk, M., Soetaert, K., van de Koppel, J., 2020. Spatial self-organization as a new perspective on cold-water coral mound development. Front. Mar. Sci. 7 https://doi.org/10.3389/fmars.2020.00631.

Van Duyl, F.C., Hegeman, J., Hoogstraten, A., Maier, C., 2008. Dissolved carbon fixation by sponge-microbe consortia of deep water coral mounds in the northeastern Atlantic Ocean. Mar. Ecol. Prog. Ser. 358, 137–150. https://doi.org/10.3354/meps07370.

Van Duyl, F.C., Scheffers, S.R., Thomas, F.I.M., Driscoll, M., 2006. The effect of water exchange on bacterioplankton depletion and inorganic nutrient dynamics in coral reef cavities. Coral Reefs 25, 23–36. https://doi.org/10.1007/s00338-005-0066-5.

Van Haren, H., Mienis, F., Duineveld, G.C.A., Lavaleye, M.S.S., 2014. High-resolution temperature observations of a trapped nonlinear diurnal tide influencing cold-water corals on the Logachev mounds. Prog. Oceanogr. 125, 16–25. https://doi.org/10.1016/j.pocean.2014.04.021.

Van Oevelen, D., Duineveld, G., Lavaleye, M., Mienis, F., Soetaert, K., Heip, C.H.R., 2009. The cold-water coral community as hotspot of carbon cycling on continental

margins: a food-web analysis from Rockall Bank (northeast Atlantic). Limnol. Oceanogr. 54, 1829–1844. https://doi.org/10.4319/lo.2009.54.6.1829.

Van Oevelen, D., Duineveld, G.C.A., Lavaleye, M.S.S., Kutti, T., Soetaert, K., 2018a. Trophic structure of cold-water coral communities revealed from the analysis of tissue isotopes and fatty acid composition. Mar. Biol. Res. 14, 287–306. https://doi.org/10.1080/17451000.2017.1398404.

Van Oevelen, D., Mueller, C.E., Lundälv, T., van Duyl, F.C., de Goeij, J.M., Middelburg, J. J., 2018b. Niche overlap between a cold-water coral and an associated sponge for isotopically-enriched particulate food sources. PloS One 13, e0194659. https://doi.org/10.1371/journal.pone.0194659.

Wagner, H., Purser, A., Thomsen, L., Jesus, C.C., Lundälv, T., 2011. Particulate organic matter fluxes and hydrodynamics at the Tisler cold-water coral reef. J. Mar. Syst. 85, 19–29. https://doi.org/10.1016/j.jmarsys.2010.11.003.

Wei, T., Simko, V., 2017. R Package "Corrplot": Visualization of a Correlation Matrix (Version 0.84). Available from. https://github.com/taiyun/corrplot.

White, M., Mohn, C., Stigter, H., Mottram, G., 2005. Deep-water Coral Development as a Function of Hydrodynamics and Surface Productivity Around the Submarine Banks of the Rockall Trough, NE Atlantic. In: Freiwald, A., Roberts, J.M. (Eds.), Cold-Water Corals and Ecosystems. Springer-Verlag Berlin Heidelberg, pp. 503–514. https://doi.org/10.1007/3-540-27673-4_25.

Wild, C., Mayr, C., Wehrmann, L., Schöttner, S., Naumann, M., Hoffmann, F., Rapp, H.T., 2008. Organic matter release by cold water corals and its implication for fauna-microbe interaction. Mar. Ecol. Prog. Ser. 372, 67–75. https://doi.org/10.3354/meps07724.

Wisshak, M., Schönberg, C.H.L., Form, A., Freiwald, A., 2014. Sponge bioerosion accelerated by ocean acidification across species and latitudes? Helgol. Mar. Res. 68, 253–262. https://doi.org/10.1007/s10152-014-0385-4.

Wright, P., 1995. Review Nitrogen Excretion: three end products, many physiological roles. J. Exp. Biol. 198, 273–281.

Wright, S.H., Manahan, D.T., 1989. Integumental nutrient uptake by aquatic organisms. Annu. Rev. Physiol. 51, 585–600. https://doi.org/10.1146/annurev.ph.51.030189.003101.

Yahel, G., Sharp, J.H., Marie, D., Häse, C., Genin, A., 2003. In situ feeding and element removal in the symbiont-bearing sponge *Theonella swinhoei*: bulk DOC is the major source for carbon. Limnol. Oceanogr. 48, 141–149.